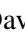





# Direct 3D Body Measurement Estimation from Sparse Landmarks

David Bojanić<sup>1</sup><sup>a</sup>, Kristijan Bartol<sup>2</sup><sup>b</sup>, Tomislav Petković<sup>1</sup><sup>c</sup> and Tomislav Pribanić<sup>1</sup><sup>d</sup>

<sup>1</sup>Faculty of Electrical Engineering and Computing, University of Zagreb, Unska 3, Zagreb, Croatia

<sup>2</sup>TU Dresden, 01062 Dresden, Dresden, Germany

**Keywords:** Anthropometry, Body Measurements, 3D Landmarks.

**Abstract:** The current state-of-the-art 3D anthropometry extraction methods are either template-based or landmark-based. Template-based methods fit a statistical human body model to a 3D scan and extract complex features from the template to learn the body measurements. The fitting process is usually an optimization process, sensitive to its hyperparameters. Landmark-based methods use body proportion heuristics to estimate the landmark locations on the body in order to derive the measurements. Length measurements are derived as distances between landmarks, whereas circumference measurements are derived as cross-sections of the body and a plane defined at the desired landmark location. This makes it very susceptible to noise in the 3D scan data. To address these issues, we propose a simple learning method that infers the body measurements directly using the landmarks defined on the body. Our method avoids fitting a body model, extracting complex features, using heuristics, and handling noise in the data. We compare our method on the CAESAR dataset and show that using a simple method coupled with sparse landmark data can compete with state-of-the-art methods. To take a step towards open-source 3D anthropometry, we make our code available at <https://github.com/DavidBoja/Landmarks2Anthropometry>.


## 1 INTRODUCTION


Anthropometry is the scientific study of the measurements and proportions of the human body (Bartol et al., 2021). With the most recent development of 3D scanners, now available even in mobile devices (Zhao et al., 2023), the need for body measurement methods from 3D data is increasing. Automatic extraction of body measurements could accelerate the tedious and time-consuming manual measurement process crucial for numerous applications such as surveying (Zakaria and Gupta, 2019), medicine (Donlić, 2019; Heymsfield et al., 2018), fashion (Zakaria and Gupta, 2019), fitness (Casadei and Kiel, 2020), and entertainment (Camba et al., 2016).


The first methods to address automatic 3D body measurement extraction were landmark-based. The goal of landmark-based methods is to extract body locations suitable for accurate measurement. These methods usually use heuristics, such as body proportions (Lu and Wang, 2008), to determine the ap-


proximate landmark locations. To further refine the landmark locations, the change in body curvature (Markiewicz et al., 2017) or the change in the cross-section by cutting the body with a plane (Zhong et al., 2018) is analyzed. Length measurements can then be estimated using the Euclidean distance or the Geodesic distance (Xie et al., 2021) between the landmarks. Circumference measurements can be determined by cutting the subject with a plane at a desired landmark, and finding the cross-section (Lu and Wang, 2008). These measurements are, however, less accurate in the presence of data noise. Additionally, such methods assume specific scanning poses (Zhong et al., 2018), no severe distortions of the body (Xie et al., 2021), known gender (Lu and Wang, 2008), etc.

Recent advances in human body measurement have been driven by statistical human body models (often referred to as templates) such as SMPL (Loper et al., 2015). The templates are relevant because body measurements can be predefined since the semantics of each vertex remain consistent across different poses and shapes (Wasenmuller et al., 2015). Template-based methods first fit a statistical body model to a 3D scan to find the optimal pose and shape parameters after which the predefined measurements

<sup>a</sup> <https://orcid.org/0000-0002-2400-0625>

<sup>b</sup> <https://orcid.org/0000-0003-2806-5140>

<sup>c</sup> <https://orcid.org/0000-0002-3054-002X>

<sup>d</sup> <https://orcid.org/0000-0002-5415-3630>

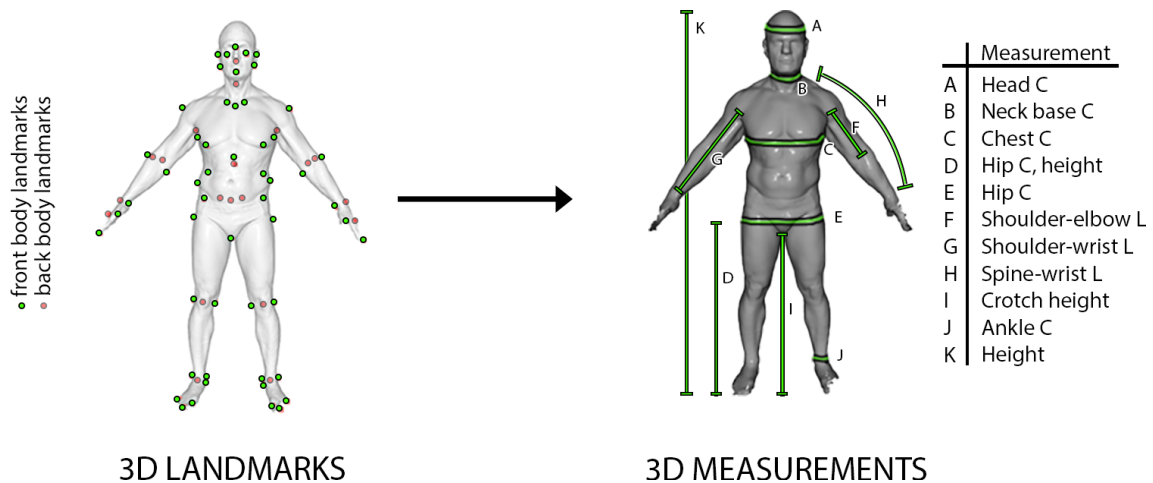


Figure 1: We use a simple Bayesian ridge model to estimate 11 body measurements (shown on the right) using 72 human body landmarks (shown on the left). We mark with green the *visible landmarks* on the front of the body, and with red the *not visible landmarks* that are located on the back of the body.

are extracted. However, the fitting is very sensitive to the hyperparameters of the minimization (Loper et al., 2015) and 3D scan data is often noisy. To increase the robustness of the body measurements, some methods extract additional features from the fitted template and use them to estimate the measurements (Yan et al., 2020). These features are complex, using multiple predefined paths or PCA coefficients of the triangle deformation found during the fitting process (Tsoli et al., 2014).

We argue that anthropometric measurements can be accurately learned using only sparse landmark data instead of complex features or heuristics. Therefore, we propose to use a simple Bayesian ridge regression model (Tipping, 2001) that takes landmark coordinates as input, and outputs body measurements. The motivation behind using the Bayesian regression model is the underlying assumption that the output variables (the measurements) are normally distributed, as can be seen in the left part of Figure 2. Furthermore, the normalized 3D coordinates of the landmarks also reflect a 3D normal distribution, as can be seen in the right part of Figure 2 (without the outliers). Using the Bayes regression, we can encode these distribution priors into the model.

Our approach assumes that accurate 3D body landmarks are given, and their automatic extraction from 3D scans is out of the scope of this work. If 3D landmarks are not given, they can be estimated using existing methods such as (Wuhrer et al., 2010; Luo et al., 2022; Xie et al., 2021). The key point is that the competing methods (Tsoli et al., 2014; Hasler et al., 2009) also assume accurate body landmarks but use them to firstly fit a template body to the 3D scan, and then estimate the body measurements, either us-

ing predefined locations or intermediate features. In contrast to previous works, we use the landmark data to directly predict the body measurements.

The main aim of our work is, therefore, to show that the fitting process and complex feature extraction can be skipped, and accurate body measurements can be estimated directly from the landmark coordinates. The body measurements estimated using only landmarks are comparable in accuracy to the body measurements obtained by first fitting the template models. To validate our claims, we evaluate our body measurement estimation approach on a public CAESAR dataset (Robinette et al., 1999).

## 2 RELATED WORK

The existing approaches for automatic body measurement extraction can typically be divided into three categories: template-based, landmark-based, and direct methods.

Landmark-based methods make use of the 3D landmarks on the body to extract the measurements from the scanned human body. To find the landmarks, (Zhong et al., 2018) slice the 3D scan every  $5mm$  along the height of the body, and search for changes in the cross-sections to find the landmarks; (Lu and Wang, 2008) use 2D silhouettes and grayscale image to detect landmarks in 2D, after which they are reprojected into the 3D space; (Xie et al., 2021) use the Mean Curvature Skeleton (Tagliasacchi et al., 2012) to find the segmentation of the body, after which heuristics are used on the segmented parts to define the landmarks; (Markiewicz et al., 2017)

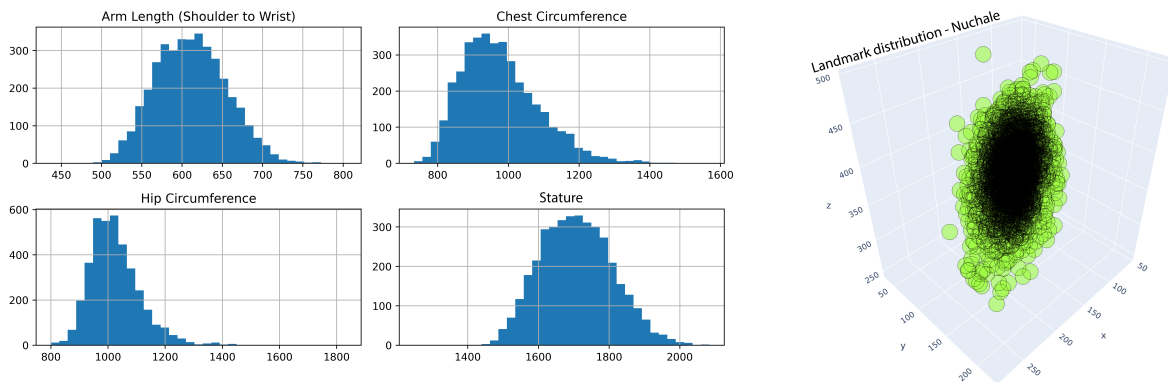


Figure 2: Distribution of measurements and landmarks. The left part of the Figure shows the distribution in mm for 4 body measurements from the CAESAR (Robinette et al., 1999) dataset: arm length (shoulder to wrist), chest circumference, hip circumference, and stature. As expected from body measurements, the arm length and stature seem to follow a normal distribution; whereas the chest and hip seem to follow a positively skewed normal distribution. The right part of the Figure shows the distribution for the Nuchale landmark over all the CAESAR dataset subjects. Since the subjects are scanned in a normalized position, the variation of the landmark location reflects the change in human body shape. The Nuchale landmarks across the subjects seem to follow a 3D normal distribution. This is observed for all the other landmarks as well.

compute the Gaussian curvature on the body to find characteristic points with salient curvatures; (Wang et al., 2006) assume colored markers on the human body during the scanning process, which they extract in post-processing. Once the landmarks are found, length measurements can be estimated as Euclidean or Geodesic distances between the landmarks, and circumference measurements can be estimated by cutting the subject with a plane at a desired landmark location and finding the cross-section. Rather than cutting the human body, (Xiaohui et al., 2018) find a path on the body mesh from a set of landmarks to determine the measurements.

Template-based methods fit a statistical human body model (template) to a 3D scan and extract complex features from the template to learn the body measurements. The fitting process can be done by optimizing over the body model parameters, and refined by non-rigid deformation (NRD) (Yan et al., 2020; Tsoli et al., 2014; Li and Paquette, 2020; Wasenmuller et al., 2015) which minimizes several loss components, such as the data term, landmark term, smoothness term and normal term. Similarly, the fitting process can be done using a deep learning model (Kaashki et al., 2021; Kaashki et al., 2023), where a 3D-CODED (Groueix et al., 2018) architecture is used to infer the fitted body. After the template body has been fitted, the measurements can be learned, transferred, or estimated from 3D landmarks. To learn the measurements (Tsoli et al., 2014; Li and Paquette, 2020; Yan et al., 2020) use 3D points and features extracted from the fitted body to learn the measurements using different models, such as the ElasticNet (Zou and Hastie, 2005), SVR (Chang and Lin, 2011) and

PLS (Geladi and Kowalski, 1986) models. To transfer the measurements (Kaashki et al., 2021; Kaashki et al., 2023; Wasenmuller et al., 2015) predefine the body measurement paths on the template body, which can be transferred onto the scan by finding the nearest neighbor of each path point from the template to the scan. Similarly, to estimate the measurements from landmarks, (Wang et al., 2014; Gonzalez Tejada and Mayer, 2020) transfer the landmarks from the template body to the scan, and find the measurement as the previously described landmark-based methods.

Differently from the template-based and landmark-based methods, direct methods (Škorvánková et al., 2022; Probst et al., 2017) learn the body measurements directly from the frontal partial 3D scans. (Škorvánková et al., 2022) uses a variation of the PointNet (Qi et al., 2016) architecture whereas (Probst et al., 2017) uses gradient-boosted trees to predict local measurements, which are weighted in order to compute the final measurements.

## 3 METHODOLOGY

### 3.1 Dataset

The CAESAR dataset (Robinette et al., 1999) is comprised of 4396 subjects scanned in the standing pose with 73 annotated body landmarks. The landmarks can be seen in Figure 3. The subjects were manually measured, and we use a subset of 11 measurements following common practice (Tsoli et al., 2014), as seen in Figure 1. We pre-process the dataset in

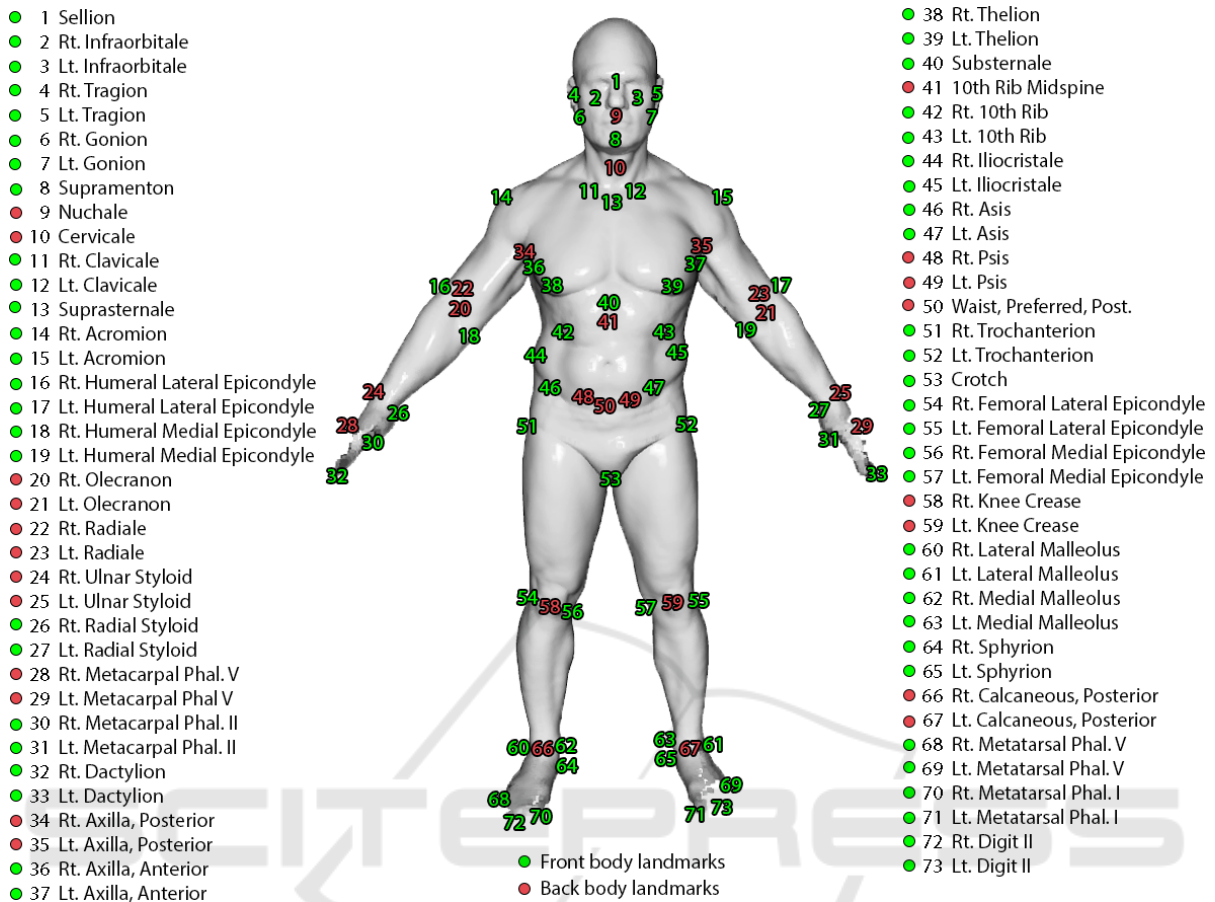


Figure 3: Landmarks used in this work defined in the CAESAR dataset. For more details, we refer the readers to (Robinette et al., 1999).

order to remove the subjects with missing landmarks or body measurements. We normalize the landmarks by centering them using the Substernale landmark located in the middle of the chest (see Figure 3). After normalization, we remove the Substernale landmark from the dataset since it does not hold any more information.

Finally, we end up with 1879 male subjects and 1954 female subjects, each with 72 landmarks and 11 body measurements. Following (Tsoli et al., 2014), we randomly sample 200 scans for each sex as a test set and use the remaining 1679 and 1754 for training.

### 3.2 Method

We use the Bayesian ridge regression model (Tipping, 2001) to learn the 11 body measurements listed in Figure 1 given the 72 body landmarks sparsely scattered over a scan. The Bayesian regression is used to include regularization parameters in the estimation procedure by introducing uninformative priors over the hyper-parameters for the precision (inverse

of variance) of the weights  $w$  and error variance  $\sigma^2$  of a linear model.

More concretely, given a set of  $N$  subjects  $\{x_n, y_n^i\}_{n=1}^N$ , where  $x_n \in \mathbb{R}^{1 \times 216}$  is the set of flattened 72 body landmarks and  $y_n^i \in \mathbb{R}^{1 \times 1}$  is the  $i$ -th body measurement, we assume a linear model:

$$y_n^i = x_n \cdot w + \epsilon_n, \quad (1)$$

where  $w \in \mathbb{R}^{216 \times 1}$  are the weights of the linear model, and  $\epsilon_n \sim \mathcal{N}(0, \sigma^2)$  is the vector of normally distributed errors. Then, the output measurement follows a Normal distribution  $p(y_n^i | x_n) = \mathcal{N}(y_n^i | x_n w, \sigma^2)$ . To use the ridge regularization, the model weights  $w$  are encoded using the normal distribution:

$$p(w | \alpha) = \prod_{i=1}^N \mathcal{N}(w_i | 0, \alpha_i^{-1}) \quad (2)$$

where  $\alpha_i$  are the hyper-parameters for the precision of each weight  $w_i$ , modeling the strength of the prior. To model these hyper-parameters, the Gamma distribution is used as a suitable conjugate prior for the preci-

Table 1: MAE in mm on the CAESAR dataset for male subjects. AE denotes the allowable error. Results from (Tsoli, 2014).

Measurement	(Anthroscan, 2014)	(Hasler et al., 2009)	(Tsoli et al., 2014)	Ours	AE (Gordon et al., 1989)
Ankle Circumference	13.66	5.72	<b>5.56</b>	6.24	4
Arm Length (Shoulder to Elbow)	13.99	12.66	13.32	<b>6.95</b>	-
Arm Length (Shoulder to Wrist)	14.49	13.76	12.66	<b>9.93</b>	-
Arm Length (Spine to Wrist)	14.71	11.81	<b>10.40</b>	11.38	-
Chest Circumference	13.96	15.21	<b>13.02</b>	18.24	15
Crotch Height	11.01	9.77	8.36	<b>1.17</b>	10
Head Circumference	<b>5.51</b>	7.46	5.59	8.92	5
Hip Circ. Max Height	<b>16.50</b>	18.89	19.05	17.33	-
Hip Circumference, Maximum	<b>7.90</b>	12.57	10.66	22.87	12
Neck Base Circumference	21.57	13.33	13.47	<b>12.40</b>	11
Stature	5.86	7.98	6.53	<b>5.75</b>	10
Average	12.65	11.74	<b>10.78</b>	11.02	

sion of the Normal distribution:

$$p(\alpha) = \prod_{i=1}^N \text{Gamma}(\alpha_i | a, b). \quad (3)$$

To model the error variance  $\sigma^2$ , the Gamma distribution is chosen as a conjugate prior for the precision:

$$p(\beta) = \text{Gamma}(\beta | c, d) \quad (4)$$

where  $\beta \equiv \sigma^{-2}$ . Higher values of the parameters  $a, b, c$  and  $d$ , indicate a stronger prior belief about the corresponding precision.

Bayesian inference proceeds by computing the posterior over all the unknowns, given the anthropometry data  $y^i = [y_1^i, \dots, y_N^i]^T$ :

$$p(w, \alpha, \sigma^2 | y^i) = \frac{p(y^i | w, \alpha, \sigma^2) p(w, \alpha, \sigma^2)}{p(y^i)}. \quad (5)$$

Equation 5 cannot be solved in full analytically because of the normalizing integral  $p(y^i)$ . Therefore, (Tipping, 2001) resort to rewriting the *posterior* as:

$$p(w, \alpha, \sigma^2 | y^i) = p(w | y^i, \alpha, \sigma^2) p(\alpha, \sigma^2 | y^i), \quad (6)$$

and using approximations, to finally summarize the problem as maximizing the *marginal likelihood*  $p(y^i | \alpha, \sigma^2) p(\alpha) p(\sigma^2)$ . These are maximized using a gradient descent approach on the *log marginal likelihood*.

Finally, given a new subject with landmarks  $x_*$ , predictions are made in terms of the distribution:

$$p(y_*^i | y^i) = \int p(y_*^i | w, \alpha, \sigma^2) p(w, \alpha, \sigma^2 | y^i) dw d\alpha d\sigma^2. \quad (7)$$

To implement the Bayesian ridge regression, we use the Scikit-learn (Pedregosa et al., 2011) library with the default values of  $1e-6$  for all the four parameters  $a, b, c$  and  $d$ . We model each measurement  $y^i$  separately, and each sex separately, resulting in  $2 \times 11 = 22$  models.

## 4 EXPERIMENTS

A great challenge with comparing and evaluating 3D anthropometric methods are the limited open-source datasets and code implementations. Most methods create private small scale dataset (Zhong et al., 2018; Kaashki et al., 2021; Lu and Wang, 2008) in order to test their method with several human body scans, and do not share it with the community because of privacy issues. Additionally, most of the methods do not share their implementations (Zhong et al., 2018; Probst et al., 2017; Tsoli et al., 2014; Lu and Wang, 2008) with the community, making a thorough comparison between different methods very hard.

We compare our method with one commercial solution denominated as Anthroscan (Anthroscan, 2014) and two template-based methods (Tsoli et al., 2014; Hasler et al., 2009), which share their results on the proprietary CAESAR dataset (Robinette et al., 1999) available for purchase. To make a step towards more open-source 3D anthropometry research, we share the exact 3D scans we evaluate our method on and make our implementation available to the research community.

We use the mean absolute error (MAE) metric to compare our estimated measurements with the ground truth ones. The MAE for a single measurement is computed as:

$$MAE = \frac{1}{N} \sum_{i=1}^N |y_{gt}^i - y_{est}^i| \quad (8)$$

where  $N$  is the number of subjects,  $y_{gt}^i$  is the ground truth measurement for subject  $i$  and  $y_{est}^i$  is the estimate measurement for subject  $i$ . We compare the MAE for each measurement separately and report them in Table 1 and Table 2.

As can be seen from Table 1 and Table 2, each method has certain advantages towards specific mea-

Table 2: MAE in mm on the CAESAR dataset for female subjects. AE denotes the allowable error. Results from (Tsoli, 2014). We bold the best result for each measurement.

Measurement	(Anthroscan, 2014)	(Hasler et al., 2009)	(Tsoli et al., 2014)	Ours	AE (Gordon et al., 1989)
Ankle Circumference	7.55	6.59	6.19	<b>5.87</b>	4
Arm Length (Shoulder to Elbow)	11.26	8.42	6.65	<b>6.32</b>	6
Arm Length (Shoulder to Wrist)	11.67	10.42	10.05	<b>7.36</b>	-
Arm Length (Spine to Wrist)	13.19	13.40	11.87	<b>9.84</b>	-
Chest Circumference	<b>12.43</b>	13.02	12.73	17.26	15
Crotch Height	7.45	7.53	5.50	<b>0.78</b>	10
Head Circumference	7.44	7.45	<b>5.91</b>	8.42	5
Hip Circ. Max Height	<b>17.05</b>	18.96	18.59	20.99	-
Hip Circumference, Maximum	<b>7.47</b>	16.15	12.35	21.40	12
Neck Base Circumference	21.03	16.35	15.43	<b>13.84</b>	11
Stature	5.60	10.21	7.51	<b>5.52</b>	10
Average	11.10	11.68	<b>10.25</b>	10.69	

measurements. The commercial solution Anthroscan (Anthroscan, 2014), achieves the lowest MAE on the hip circumference measurements for both female and male subjects. The reason for this might be that the measurements are directly extracted from dense scan data, without using a body template or relying on accurate landmark data. However, the method achieves the worst average results when comparing all the measurements, making it less robust for human shape estimation. The template-based method from (Hasler et al., 2009) performs slightly better (on average) than Anthroscan. However, it does not seem to have any advantages towards any specific measurement. (Hasler et al., 2009) fits the template of the SCAPE (Anguelov et al., 2005) body model onto the scan, and uses a linear model to predict the measurements from the body model vertices. This kind of approach, however, depends on a very sensitive, initial fitting process, since the measurements are then extracted from the template.

To address these issues, (Tsoli et al., 2014) fits a BlendSCAPE (Hirshberg et al., 2012) body model to the 3D scan and extracts complex features from the template to learn an ElasticNet (Zou and Hastie, 2005) linear model to predict the measurements. By using more sophisticated features, such as a set of pre-defined paths, PCA coefficients of the body model fitting, and limb lengths, (Tsoli et al., 2014) achieves better results than the previous methods because, in the end, it considers a much greater number of local and global features. As can be seen from the Tables, they achieve the lowest average errors.

We argue that dense 3D data and an additional set of features are not necessary to accurately estimate the body measurements and, therefore, we propose using only the 3D landmark data to estimate the measurements. As shown in Table 1 and 2, using only sparse landmark data, our method achieves comparable results to the state-of-the-art methods while

simplifying the measurement protocol. The method achieves the best performance on the length measurements, such as arm lengths, crotch height, and stature for both sexes. Intuitively, these measurements benefit from using landmarks, which are directly correlated to how they are manually measured. Consequently, our method achieves the lowest error on the neck base circumference, which is the second hardest measurement to estimate, judging by the average errors across all of the competing methods. When measured manually by the experts, the neck base circumference is taken with a beaded chain with an alligator clip at one end. The chain is placed and clipped together so it lies at the base of the neck and falls over the Cervicale landmark (see Figure 3). The length of the chain to the bead where it is clipped is measured. This measuring protocol differs severely from the others, making the measurement harder to estimate. Our method seems to benefit, again, from well-placed landmarks around the neck area, allowing a better estimate of the measurement.

On the other hand, our method seems to struggle with the chest and hip circumferences. One reason for this can be attributed to the location of the landmarks. With manual measurement, the chest circumference is located on the largest part between the Thelion and Axilla landmarks. As can be seen from Figure 3, however, there are no landmarks in that location. Similarly, with manual measurement, the hip circumference is located at the maximum protrusion of the buttocks, approximately around the Trochantion landmarks. As can be seen from Figure 3, again, there are no landmarks on the front and back of the body in those locations, which we know carry a lot of variation of the human shape. Therefore, our method needs to infer these measurements from substantially less information than the competing methods (sparse landmarks) and use the spatial relationship between all the other landmarks, to infer the body proportions.

The second reason these measurements are harder to estimate is the assumption of the Bayesian regression to model the output variable (the measurements) with the Normal distribution. As can be seen from Figure 2, the chest and hip circumferences are the only two measurements that have slightly skewed normal distributions, making them harder to generalize. To address these issues, future work should focus on landmark placement, making them more informative. Rather than using multiple landmarks on the feet of the subjects, for example, they could be replaced with landmarks around the chest and hip area.

Finally, our average measurements for the male and female subjects are behind the state-of-the-art method from (Tsoli et al., 2014) by only 0.24 mm and 0.44 mm respectively. We note, however, that our average MAE gets skewed by the higher hip and chest circumference errors. Comparing the median errors, on the other hand, our method would achieve a median MAE of 9.93 mm for the male subjects, compared to 10.66 mm from (Tsoli et al., 2014); and a median MAE of 8.42 mm for the female subjects, compared to 10.05 mm from (Tsoli et al., 2014). Therefore, addressing the issue of better landmark placement would greatly improve our results.

## 5 CONCLUSION

We propose a simple 3D body measurement estimation method directly using the landmarks on the body. Our method shows better or comparable results on the CAESAR dataset for most measurements, and achieves the lowest errors on the arm lengths, crotch height, stature, and neck base circumference, for both sexes. With our method, we show that extracting complex features prior to measuring (such as multiple paths from the fitted template model, or PCA coefficients of the triangle deformation of the fitted template model), is not necessary to accurately estimate the body measurements. Additionally, we show that fitting a template body model to the scan is also not necessary if given the location of 3D landmarks; where accurate measurements can be directly estimated from the landmarks.

To further improve the results for certain measurements, such as the hip and chest circumferences, future work will need to address the placement of the 3D landmarks, in order to provide the model with additional information about the body shape. By coupling the accurate landmark placement with a 3D landmark extraction algorithm, our 3D body measurement method could be made fully automatic.

## ACKNOWLEDGEMENTS

This work has been supported by the Croatian Science Foundation under projects IP-2018-01-8118 and DOK-2020-01.

## REFERENCES

- Anguelov, D., Srinivasan, P., Koller, D., Thrun, S., Rodgers, J., and Davis, J. (2005). Scape: Shape completion and animation of people. *ACM Trans. Graph.*, 24(3):408–416.
- Anthroscan (2014). Human solutions gmbh. anthroscan. <http://www.https://www.human-solutions.com/>. Accessed: 2023-10-06.
- Bartol, K., Bojanić, D., Petković, T., and Pribanić, T. (2021). A review of body measurement using 3d scanning. *IEEE Access*, 9:67281–67301.
- Camba, J. D., De Leon, A. B., de la Torre, J., Saorín, J. L., and Contero, M. (2016). Application of low-cost 3d scanning technologies to the development of educational augmented reality content. In *2016 IEEE Frontiers in Education Conference (FIE)*, pages 1–6.
- Casadei, K. and Kiel, J. (2020). *Anthropometric Measurement*. StatPearls Publishing, Treasure Island (FL).
- Chang, C.-C. and Lin, C.-J. (2011). LIBSVM. *ACM Transactions on Intelligent Systems and Technology*, 2(3):1–27.
- Donlić, M. (2019). *Three-dimensional analysis of back surface under dynamic conditions in scoliosis diagnostics*. PhD thesis, Faculty of Electrical Engineering and Computing, University of Zagreb.
- Geladi, P. and Kowalski, B. R. (1986). Partial least-squares regression: a tutorial. *Analytica Chimica Acta*, 185:1–17.
- Gonzalez Tejada, Y. and Mayer, H. A. (2020). Calvis: chest, waist and pelvis circumference from 3d human body meshes as ground truth for deep learning.
- Gordon, C. C., Churchill, T., Clauser, C. E., Bradtmiller, B., and Mcconville, J. T. (1989). Anthropometric survey of u.s. army personnel: Methods and summary statistics 1988.
- Groueix, T., Fisher, M., Kim, V. G., Russell, B., and Aubry, M. (2018). 3d-coded : 3d correspondences by deep deformation. In *ECCV*.
- Hasler, N., Stoll, C., Sunkel, M., Rosenhahn, B., and Seidel, H.-P. (2009). A Statistical Model of Human Pose and Body Shape. *Computer Graphics Forum*.
- Heymsfield, S. B., Bourgeois, B., Ng, B. K., Sommer, M. J., Li, X., and Shepherd, J. A. (2018). Digital anthropometry: a critical review. *European journal of clinical nutrition*, 72(5):680–687.
- Hirshberg, D. A., Loper, M., Rachlin, E., and Black, M. J. (2012). Coregistration: Simultaneous alignment and modeling of articulated 3d shape. In *Computer Vision – ECCV 2012*, pages 242–255. Springer Berlin Heidelberg.

- Kaashki, N. N., Hu, P., and Munteanu, A. (2021). Deep learning-based automated extraction of anthropometric measurements from a single 3-d scan. *IEEE Transactions on Instrumentation and Measurement*, 70:1–14.
- Kaashki, N. N., Hu, P., and Munteanu, A. (2023). Anet: A deep neural network for automatic 3d anthropometric measurement extraction. *IEEE Transactions on Multimedia*, 25:831–844.
- Li, P. and Paquette, S. (2020). Predicting anthropometric measurements from 3d body scans: Methods and evaluation. In Di Nicolantonio, M., Rossi, E., and Alexander, T., editors, *Advances in Additive Manufacturing, Modeling Systems and 3D Prototyping*, pages 561–570, Cham. Springer International Publishing.
- Loper, M., Mahmood, N., Romero, J., Pons-Moll, G., and Black, M. J. (2015). SMPL: A skinned multi-person linear model. *ACM Trans. Graphics (Proc. SIGGRAPH Asia)*, 34(6):248:1–248:16.
- Lu, J. and Wang, M. (2008). Automated anthropometric data collection using 3d whole body scanners. *Expert Systems with Applications*, 35(1-2):407–414.
- Luo, S., Zhang, Q., and Feng, J. (2022). Automatic location and semantic labeling of landmarks on 3d human body models. *Computational Visual Media*, 8(4):553–570.
- Markiewicz, Ł., Witkowski, M., Sitnik, R., and Mielicka, E. (2017). 3d anthropometric algorithms for the estimation of measurements required for specialized garment design. *Expert Systems with Applications*, 85:366–385.
- Pedregosa, F., Varoquaux, G., Gramfort, A., Michel, V., Thirion, B., Grisel, O., Blondel, M., Prettenhofer, P., Weiss, R., Dubourg, V., Vanderplas, J., Passos, A., Cournapeau, D., Brucher, M., Perrot, M., and Duchesnay, E. (2011). Scikit-learn: Machine learning in Python. *Journal of Machine Learning Research*, 12:2825–2830.
- Probst, T., Fossati, A., Salzmann, M., and Gool, L. V. (2017). Efficient model-free anthropometry from depth data. In *2017 International Conference on 3D Vision (3DV)*. IEEE.
- Qi, C. R., Su, H., Mo, K., and Guibas, L. J. (2016). Pointnet: Deep learning on point sets for 3d classification and segmentation. *arXiv preprint arXiv:1612.00593*.
- Robinette, K. M., Daanen, H., and Paquet, E. (1999). The caesar project: a 3-d surface anthropometry survey. In *Second International Conference on 3-D Digital Imaging and Modeling (Cat. No.PR00062)*, pages 380–386.
- Škorvánková, D., Riečický, A., and Madaras, M. (2022). Automatic estimation of anthropometric human body measurements. In *Proceedings of the 17th International Joint Conference on Computer Vision, Imaging and Computer Graphics Theory and Applications*. SCITEPRESS - Science and Technology Publications.
- Tagliasacchi, A., Alhashim, I., Olson, M., and Zhang, H. (2012). Mean curvature skeletons. *Computer Graphics Forum*, 31(5):1735–1744.
- Tipping, M. E. (2001). Sparse bayesian learning and the relevance vector machine. *J. Mach. Learn. Res.*, 1:211–244.
- Tsoli, A. (2014). *Modeling the Human Body in 3D: Data Registration and Human Shape Representation*. PhD thesis, Brown University, Department of Computer Science.
- Tsoli, A., Loper, M., and Black, M. J. (2014). Model-based anthropometry: Predicting measurements from 3d human scans in multiple poses. In *IEEE Winter Conference on Applications of Computer Vision*. IEEE.
- Wang, M.-J. J., Wu, W.-Y., Lin, K.-C., Yang, S.-N., and Lu, J.-M. (2006). Automated anthropometric data collection from three-dimensional digital human models. *The International Journal of Advanced Manufacturing Technology*, 32(1-2):109–115.
- Wang, Q., Jagadeesh, V., Ressler, B., and Piramuthu, R. (2014). Im2fit: Fast 3d model fitting and anthropometrics using single consumer depth camera and synthetic data. In *3D Image Processing, Measurement, and Applications*.
- Wasenmuller, O., Peters, J. C., Golyanik, V., and Stricker, D. (2015). Precise and automatic anthropometric measurement extraction using template registration. In *Proceedings of the 6th International Conference on 3D Body Scanning Technologies, Lugano, Switzerland, 27-28 October 2015*. Hometrica Consulting - Dr. Nicola D'Apuzzo.
- Wuhrer, S., Azouz, Z. B., and Shu, C. (2010). Semi-automatic prediction of landmarks on human models in varying poses. In *2010 Canadian Conference on Computer and Robot Vision*, pages 136–142.
- Xiaohui, T., Xiaoyu, P., Liwen, L., and Qing, X. (2018). Automatic human body feature extraction and personal size measurement. *Journal of Visual Languages & Computing*, 47:9–18.
- Xie, H., Zhong, Y., Yu, Z., Hussain, A., and Chen, G. (2021). Automatic 3d human body landmarks extraction and measurement based on mean curvature skeleton for tailoring. *The Journal of The Textile Institute*, 113(8):1677–1687.
- Yan, S., Wirta, J., and Kämäräinen, J.-K. (2020). Anthropometric clothing measurements from 3d body scans. *Machine Vision and Applications*, 31(1-2).
- Zakaria, N. and Gupta, D. (2019). *Anthropometry, Apparel Sizing and Design*. The Textile Institute Book Series. Elsevier Science.
- Zhao, H., Chen, J., Wang, L., and Lu, H. (2023). Arkitrack: A new diverse dataset for tracking using mobile rgb-d data. In *Proceedings of the IEEE/CVF Conference on Computer Vision and Pattern Recognition (CVPR)*, pages 5126–5135.
- Zhong, Y., Li, D., Wu, G., and Hu, P. (2018). Automatic body measurement based on slicing loops. *International Journal of Clothing Science and Technology*, 30(3):380–397.
- Zou, H. and Hastie, T. (2005). Regularization and variable selection via the elastic net. *Journal of the Royal Statistical Society Series B: Statistical Methodology*, 67(2):301–320.